

Article

Cobalt and Iron Cyano Benzene Bis(Dithiolene) Complexes

António G. Costa ¹, Gonçalo Lopes ¹, João F. G. Rodrigues ¹, Isabel C. Santos ¹ , Dulce Simão ² , Elsa B. Lopes ¹ ,
Laura C. J. Pereira ¹ , Nolwenn Le Breton ³, Sylvie Choua ³, Stéphane A. Baudron ⁴ , Manuel Almeida ¹ 
and Sandra Rabaça ^{1,*} 

¹ Centro de Ciências e Tecnologias Nucleares (C2TN), Associação do Instituto Superior Técnico para a Investigação e Desenvolvimento (IST-ID), Departamento de Engenharia e Tecnologias Nucleares (DECN), Instituto Superior Técnico (IST), Universidade de Lisboa, Estrada Nacional 10, 2695-066 Bobadela, Portugal; antonio.costa@ctn.tecnico.ulisboa.pt (A.G.C.); eblopes@ctn.tecnico.ulisboa.pt (E.B.L.); lpereira@ctn.tecnico.ulisboa.pt (L.C.J.P.)

² Centro de Química Estrutural (CQE), Associação do Instituto Superior Técnico para a Investigação e Desenvolvimento (IST-ID), Departamento de Engenharia Química (DEQ), Instituto Superior Técnico (IST), Universidade de Lisboa, Av. Rovisco Pais, 1049-001 Lisboa, Portugal; dulcesimao@tecnico.ulisboa.pt

³ Institut de Chimie, UMR CNRS 7177, Université de Strasbourg, Institut Le Bel, 4 Rue Blaise Pascal, CS 90032, 67081 Strasbourg, France

⁴ CNRS, CMC UMR 7140, Université de Strasbourg, 4 rue Blaise Pascal, 67000 Strasbourg, France; sbaudron@unistra.fr

* Correspondence: sandrar@ctn.tecnico.ulisboa.pt

Abstract: New iron and cobalt bis(dithiolene) complexes [M(3cbdt)₂] (3cbdt = 3-cyanobenzene-1,2-dithiolate) were prepared as tetraphenylphosphonium (Ph₄P⁺) salts for Fe in the monoanionic state and for Co in both the dianionic and monoanionic states: (Ph₄P)₂[Fe(III)(3cbdt)₂]₂ (**1**); (Ph₄P)₂[Co(III)(3cbdt)₂]₂ (**2**); (Ph₄P)₂[Co(II)(3cbdt)₂] (**3**). These compounds were characterized by single-crystal X-ray diffraction, cyclic voltammetry, EPR, and static magnetic susceptibility. Their properties are discussed in comparison with the corresponding complexes based on the isomer ligand 4-cyanobenzene-1,2-dithiolate (4cbdt) and 4,5-cyanobenzene-1,2-dithiolate (dcbdt), previously described by us. The Fe(III) and the Co(III) compounds (**1** and **2**) are isostructural, crystallizing in the triclinic $P\bar{1}$ space group, with cis [M(III)(3cbdt)₂] complexes dimerized in a trans fashion, and the transition metal (M = Fe, Co) has a distorted 4+1 square pyramidal coordination geometry. The Co(II) compound (**3**) crystallizes in the triclinic $P\bar{1}$ space group, with the unit cell containing one cis and three trans inequivalent [Co(II)(3cbdt)₂] complexes with the transition metal (Co) and having a square planar coordination geometry. The Fe(III) complex (**1**) is EPR-silent, and the static magnetic susceptibility shows a temperature dependence typical of dimers of antiferromagnetically coupled $S = 3/2$ spins with $-J/k_B = 233.6$ K and $g = 1.8$. Static magnetic susceptibility measurements of compound (**3**) show that this Co(II) complex is paramagnetic, corresponding to an $S = 1/2$ state with $g = 2$, in agreement with EPR spectra showing in solid state a hyperfine structure typical of the $I(^{59}\text{Co}) = 7/2$. Static susceptibility measurements of Co(III) complex (**2**) showed an increase in the paramagnetic susceptibility upon warming above 100 K, which is consistent with strong AFM coupling between dimerized $S = 1$ units with a constant $-J/k_B \sim 1286$ K.

Keywords: bis(dithiolene) metal transition complexes; thio-azo ligands; cobalt; iron; crystal structure; cyclic voltammetry; magnetic properties; electron paramagnetic resonance



Citation: Costa, A.G.; Lopes, G.; Rodrigues, J.F.G.; Santos, I.C.; Simão, D.; Lopes, E.B.; Pereira, L.C.J.; Le Breton, N.; Choua, S.; Baudron, S.A.; et al. Cobalt and Iron Cyano Benzene Bis(Dithiolene) Complexes. *Crystals* **2024**, *14*, 469. <https://doi.org/10.3390/cryst14050469>

Academic Editor: Alexander Y. Nazarenko

Received: 16 April 2024

Revised: 7 May 2024

Accepted: 14 May 2024

Published: 17 May 2024



Copyright: © 2024 by the authors. Licensee MDPI, Basel, Switzerland. This article is an open access article distributed under the terms and conditions of the Creative Commons Attribution (CC BY) license (<https://creativecommons.org/licenses/by/4.0/>).

1. Introduction

Transition-metal dithiolene complexes have been attracting continuous attention for more than 50 years [1–5], becoming a large class of compounds increasingly relevant both for fundamental studies in coordination chemistry and in different fields and applications from materials science [6,7], catalysis [8], bioinorganic chemistry [9–11], energy conversion [12–14] and biological systems [15]. In spite of a quite long and extensive research

history, these compounds continue to be studied, with novel families being frequently identified and providing revitalizing sources of interest [16].

A key feature of the bis(dithiolene) complexes is their capability to assume different oxidation states. The vivid redox behavior of many of these complexes is due to a significant contribution of the ligands to the frontier orbitals, playing the so-called non-innocent role in ligand-centered redox processes [17–19]. The possibility to obtain complexes in different oxidation states and with different metals provides access to different magnetic moments constituting useful degrees of freedom in the design of the magnetic properties of molecular materials.

As a general tendency, the monoanionic state is the most stable within bis(dithiolene) complexes. Dianionic states are also frequently obtained and, in some cases, are neutral complexes, or in even higher oxidation states, they can be isolated in stable compounds. Furthermore, the electroactive character of these complexes frequently permits the existence of persistent partially oxidized states. Recent developments have spotlighted instances where these complexes, while in their neutral state, manifest remarkable electrical conductivity and authentic metallic characteristics [18–20].

The d-metal dithiolene complexes also present a very rich structural diversity. Most studies have been focused on transition metals such as Au, Ni, Pd, Pt, Cu, Ag, or Zn, and among about 2568 entries in the CCDC database, the square planar coordination geometry is dominant, and only 169 entries refer to Co and Fe. For Fe, a dimeric arrangement of Fe bis(dithiolene) monoanionic units with a (4+1) square pyramidal coordination is the prevailing norm, with only two exceptional cases: (*n*-Bu₄N) [Fe(qdt)₂] (qdt = 2,3-quinoxalinedithiolate) [21] and [Fe(S₂C₂(*p*-anisyl)₂)] [22], where this dimerization could be prevented due to specific solid-state interactions and a square planar geometry being observed.

For Co, a larger structural diversity has been observed, with the dimerization being less favored. In addition to the square planar geometry, bis(dithiolene) complexes are known to adopt also dimeric [23,24], trimeric [25], and even polymeric [26] arrangements due to the formation of extra apical Co over S bonds.

Previously, we focused our attention on transition-metal bis(dithiolene) complexes with cyano benzene ligands and reported extensive studies of two families of complexes: [M(dcbdt)₂] [24,27–32] and [M(4cbdt)₂] [33,34], with different d-metals M = Zn, Ni, Pd, Pt, Co, Cu, Fe, Au). Here, dcbdt (dicyanobenzene-1,2-dithiolate) and 4cbdt (4-cyanobenzene-1,2-dithiolate) were employed as ligands (Figure 1). The incorporation of cyano groups into dithiolene ligands is regarded as an interesting tool for tailoring the physical properties of these complexes. The number and position of electron-withdrawing groups (–C≡N) on both the dithiolene complexes as well as in the analogous TTF donors [35–37] are known to considerably influence their redox characteristics. In addition, these cyano moieties offer secondary coordination possibilities for constructing more complex heterometallic coordination architectures and networks [38–45] and may also provide –C≡N⋯H interactions, promoting distinctive structural motifs in the solid state.

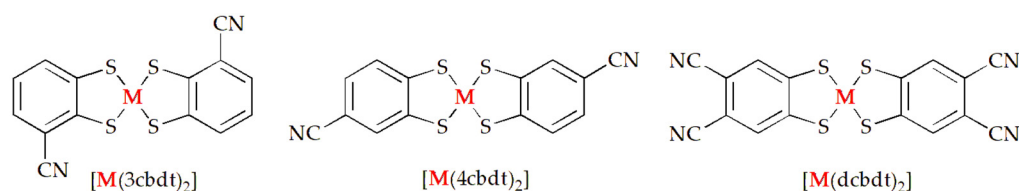


Figure 1. Molecular scheme of the cyano benzene bis(dithiolene) metal complexes [M(3cbdt)₂], [M(4cbdt)₂] and [M(dcbdt)₂].

More recently, we reported the nickel and copper complexes [M(3cbdt)₂]^{Z−} (Z = 1, 2 and M = Ni, Cu) [46] as the first two members of a new family of bis(dithiolene) complexes with a new isomer of the cyano benzene dithiolene ligand, 3-cyanobenzene-1,2-dithiolate. In this work, we report the iron and cobalt complexes with this ligand, [Fe(3cbdt)₂] and [Co(3cbdt)₂], which were obtained as tetraphenylphosphonium salts for Fe in the monoan-

ionic state and for Co in both the dianionic and monoanionic states, with the last one being isostructural to the Fe analog. The monoanionic complexes present dimerization with a distorted square pyramidal 4 + 1 metal coordination geometry.

2. Materials and Methods

2.1. General Information

The 2-oxobenzod[1,3]dithiole-4-carbonitrile [37] was synthesized following previously published procedures, and all the other reagents were purchased from commercial sources and used without any additional purification.

2.2. Synthesis

(Ph₄P)₂[Fe(3cbdt)₂]₂·2CH₂Cl₂ (**1**). Initially, 2-oxobenzod[1,3]dithiole-4-carbonitrile (100 mg, 0.52 mmol) was dissolved in a NaOH solution (100 mg, 2.5 mmol) in 10 mL of H₂O/EtOH (1:1) using a water bath at 50 °C. Within 10 min of stirring, the solution turned clear yellow. Subsequently, a solution of FeCl₃ (46 mg, 0.267 mmol) in 5 mL of H₂O/EtOH (1:1) was added. After stirring for 5 min, a solution of Ph₄PBr (250 mg, 0.59 mmol) in 10 mL of H₂O/EtOH (1:1) was introduced. The solution was then left overnight at low temperatures (between 0 °C and 7 °C). The resulting brown precipitate was filtered, washed with cold methanol, and dried. Finally, the compound was recrystallized in CH₂Cl₂/hexane, yielding black crystals after 1 week. (103 mg, 0.072 mmol, 55.38%). M.p. 300 °C; FTIR (cm⁻¹): ν = 3050 (w, Ar-H), 2212 (s, C≡N), 1550–1482 (m, C=C); ESI-MS: (+) obs. *m/z* 339.2, calcd. *m/z* 339.130 ((Ph₄P)⁺, 100%); (−) obs. *m/z* 771.8, calcd. *m/z* 771.75 ([Fe(3cbdt)₂]₂^{2−}, 100%); Anal. calcd for C₇₈H₅₆Cl₄Fe₂N₄P₂S₈ (1621.28): C 57.78, H 3.48, N 3.46, S 15.82. Found: C 58.12, H 3.57, N 3.68, S 16.12.

(Ph₄P)₂[Co(3cbdt)₂]₂·2CH₂Cl₂ (**2**). Following a similar procedure as used for **1** but with a solution of CoCl₂·6H₂O (64 mg, 0.26 mmol) instead of FeCl₃, **2** was obtained as black needles (95 mg, 0.069 mmol, 53.07%). M.p. 201–203 °C; FTIR (cm⁻¹): ν = 3057 (w, Ar-H), 2210 (s, C≡N), 1560–1492 (m, C=C); ESI-MS: (+) obs. *m/z* 339.2, calcd. *m/z* 339.130 ((Ph₄P)⁺, 100%); (−) obs. *m/z* 777.7, calcd. *m/z* 777.75 ([Co(3cbdt)₂]₂^{2−}, 100%); Anal. calcd for C₇₈H₅₆Cl₄Co₂N₄P₂S₈ (1627.45): C 57.56, H 3.47, N 3.44, S 15.76. Found: C 57.82, H 3.10, N 3.49, S 16.20.

(Ph₄P)₂[Co(3cbdt)₂] (**3**). Under a nitrogen atmosphere, 2-oxobenzod[1,3]dithiole-4-carbonitrile (100 mg, 0.52 mmol) was dissolved in a MeONa solution (90 mg, 1.6 mmol) in 2 mL of MeOH. The solution turned clear yellow within 5 min of stirring. Subsequently, a solution of CoCl₂·6H₂O (64 mg, 0.26 mmol) in 2 mL of MeOH was prepared and added to the previous solution. After stirring for 5 min, a Ph₄PBr (0.22 mg, 0.52 mmol) solution in 2 mL of the same solvent was added to this mixture. The solution was left to stand for 2 days at low temperatures (between 0 °C and 7 °C), resulting in the formation of needle-shaped blue crystals (80 mg, 0.075 mmol, 28.9% yield). M.p. 170–171 °C; FTIR (cm⁻¹): ν = 3042 (w, Ar-H), 2213 (s, C≡N), 1583–1482 (m, C=C); ESI-MS: (+) obs. *m/z* 339.2, calcd. *m/z* 339.130 ((Ph₄P)⁺, 100%); (−) obs. *m/z* 388.7, calcd. *m/z* 388.87 ([Co(3cbdt)₂][−], 100%); Anal. calcd for C₆₂H₄₆CoN₂P₂S₄ (1068.18): C 69.71, H 4.34, N 2.62, S 12.01 Found: C 70.10, H 4.23, N 2.75, S 12.41.

2.3. X-ray Crystallography

Crystals of **1–3** were prepared for analysis by mounting them on a cryoloop immersed in FOMBLIM protective oil. Data collection was performed using a Bruker D8 QUEST diffractometer equipped with graphite-monochromated Mo K α radiation ($\alpha = 0.71073$ Å) in φ and ω scan modes, with data acquisition managed by the APEX3 program [47]. The unit cell parameters were determined using Bruker SMART software (Version 6.45) and refined using the Bruker SAINT program applied to all observed reflections [48]. Empirical absorption corrections were applied using SADABS [49]. Structure solutions were achieved through direct methods utilizing SHELXT [50], followed by full-matrix least-squares refinement against F² using SHELXL [51], which is integrated into the WINGX

program package [52]. Most non-hydrogen atoms were refined with anisotropic thermal parameters, while hydrogen atoms were positioned at idealized locations and allowed to refine in relation to their parent carbon atoms. Molecular visualizations were generated using Mercury [53]. The supplementary crystallographic data for this paper can be accessed via the Cambridge Crystallographic Data Centre (CCDC) deposition numbers 2346079, 23406080, and 23406081, available for free download at www.ccdc.cam.ac.uk/data_request/cif, accessed on 16 April 2024. Crystallographic data for compounds 1–3 are summarized in Table 1.

Table 1. Crystallographic data for compounds 1–3.

Compound	(Ph ₄ P) ₂ [Fe(3cbdt) ₂] ₂ 2CH ₂ Cl ₂ (1)	(Ph ₄ P) ₂ [Co(3cbdt) ₂] ₂ 2CH ₂ Cl ₂ (2)	(Ph ₄ P) ₂ [Co(3cbdt) ₂] (3)
Empirical formula	C ₇₈ H ₅₆ Cl ₄ Fe ₂ N ₄ P ₂ S ₈	C ₇₈ H ₅₆ Cl ₄ Co ₂ N ₄ P ₂ S ₈	C ₆₂ H ₄₆ Co N ₂ P ₂ S ₄
Crystal size (mm)	0.180 × 0.100 × 0.040	0.450 × 0.180 × 0.040	0.400 × 0.020 × 0.020
Molecular mass (g/mol)	1621.18	1627.34	1068.12
Temperature (K)	150 (2)	273 (2)	294 (2)
Crystal system	Triclinic	Triclinic	Triclinic
Space group	<i>P</i> $\bar{1}$	<i>P</i> $\bar{1}$	<i>P</i> $\bar{1}$
<i>a</i> (Å)	11.2179 (9)	11.2465 (6)	14.0437 (7)
<i>b</i> (Å)	13.6086 (10)	13.6794 (7)	22.4513 (13)
<i>c</i> (Å)	13.6118 (10)	13.7567 (7)	26.2961 (15)
α (°)	108.102 (3)	108.146 (2)	88.930 (2)
β (°)	103.708 (3)	100.930 (2)	78.425 (2)
γ (°)	100.865 (3)	103.540 (2)	87.578 (2)
<i>V</i> (Å ³)	1839.9 (2)	1874.65 (17)	8114.8 (8)
<i>Z</i> , <i>D</i> _{calcd} (Mg/m ³)	1, 1.463	1, 1.441	6, 1.311
μ (mm ⁻¹)	0.858	0.897	0.572
<i>F</i> (000)	830	832	3318
θ Range (°)	2.644 to 25.680	1.943 to 27.164	2.910 to 25.682
Index range (<i>h,k,l</i>)	−8 ≤ <i>h</i> ≤ 13, −16 ≤ <i>k</i> ≤ 15, −16 ≤ <i>l</i> ≤ 16	−14 ≤ <i>h</i> ≤ 14, −17 ≤ <i>k</i> ≤ 17, −16 ≤ <i>l</i> ≤ 17	−17 ≤ <i>h</i> ≤ 15, −27 ≤ <i>k</i> ≤ 26, −32 ≤ <i>l</i> ≤ 32
Reflections collected/unique (<i>R</i> _{int})	16,844/6888 (0.1459)	30,409/8289 (0.0829)	64,280/29,898 (0.2535)
<i>T</i> _{max/min.} GOOF on <i>F</i> ²	0.967 and 0.861 0.900	0.965 and 0.688 1.062	0.989 and 0.803 0.825
Final <i>R</i> ₁ , [<i>I</i> > 2σ(<i>I</i>)], <i>wR</i> ₂ CCDC	<i>R</i> ₁ = 0.0821, <i>wR</i> ₂ = 0.1409 2346079	<i>R</i> ₁ = 0.0610, <i>wR</i> ₂ = 0.1544 23406080	<i>R</i> ₁ = 0.0945, <i>wR</i> ₂ = 0.1375 23406081

2.4. Cyclic Voltammetry Studies

Cyclic voltammetry data were obtained using a BAS C3 Cell Stand. The voltammograms were obtained at room temperature with variable scan rates in the range of 50–500 mV s⁻¹, using platinum wire working, counter electrodes, and an Ag/AgNO₃ (0.01 M AgNO₃ and 0.1 M *n*Bu₄NPF₆ in acetonitrile) reference electrode, in which the Ag⁺ ion electrode was separated from the bulk solution by a Vycor™ frit. The measurements were performed on fresh solutions with a concentration of ~0.5 × 10⁻³ M in acetonitrile, which contained *n*-Bu₄NPF₆ (0.1 M) as a supporting electrolyte. Ferrocene was added directly to the solution after cyclic voltammogram registration to allow for the potential normalization in situ, relative to the ferrocene/ferrocenium couple redox potential that was found to be at *E*_{1/2} = 0.36 V vs. Ag/AgNO₃.

2.5. Magnetic Susceptibility Measurements

Magnetic susceptibility measurements were conducted on polycrystalline samples weighing approximately 10–15 mg each. These measurements were performed using a 7 Tesla S700X SQUID magnetometer manufactured by Cryogenic Ltd., (London, UK) over a temperature range of 4 to 300 K, and with an applied magnetic field of 1 T. Paramagnetic susceptibility values were derived from the raw data and adjusted for sample holder contri-

butions, incorporating a diamagnetic correction based on tabulated Pascal constants, yielding values of -832×10^{-6} emu/mol, -832×10^{-6} emu/mol and -665×10^{-6} emu/mol for $(\text{Ph}_4\text{P})_2[\text{Fe}(\text{3cbdt})_2]_2$, $(\text{Ph}_4\text{P})_2[\text{Co}(\text{3cbdt})_2]_2$ and $(\text{Ph}_4\text{P})_2[\text{Co}(\text{3cbdt})_2]$, respectively.

2.6. EPR Spectrometry

EPR spectra were recorded on an EMX spectrometer (Bruker Biospin GmbH, Ettlingen, Germany) operating at X-band, equipped with a high sensitivity resonator (ER4119HS, Bruker, Ettlingen, Germany) and a variable temperature unit (ER4131VT, Bruker). Spectra were simulated using Easyspin 6.0.0-dev.54.

2.7. Mass Spectrometry

Mass spectra were obtained by electrospray ionization (ESI-MS) in a Bruker HCT quadrupole ion trap mass spectrometer (Bruker Daltonics GmbH, Bremen, Germany).

3. Results

3.1. Tetraphenylphosphonium Bis(Dithiolene) Complexes Synthesis

The $[\text{Fe}(\text{3cbdt})_2]^-$ and $[\text{Co}(\text{3cbdt})_2]^{2-/-}$ complexes were obtained as tetraphenylphosphonium salts, from the proligand 2-oxobenzo[d][1,3]dithiole-4-carbonitrile (**A**) prepared as previously described [37], following procedures similar to those recently described for preparing the Ni and Cu complexes. [46] The benzothioxo **A** was reacted in a basic medium with chloride salts of cobalt or iron, and the resulting metal bis(dithiolene) complexes precipitated as tetraphenylphosphonium salts upon the addition of $(\text{Ph}_4\text{P})\text{Br}$ (Figure 2).

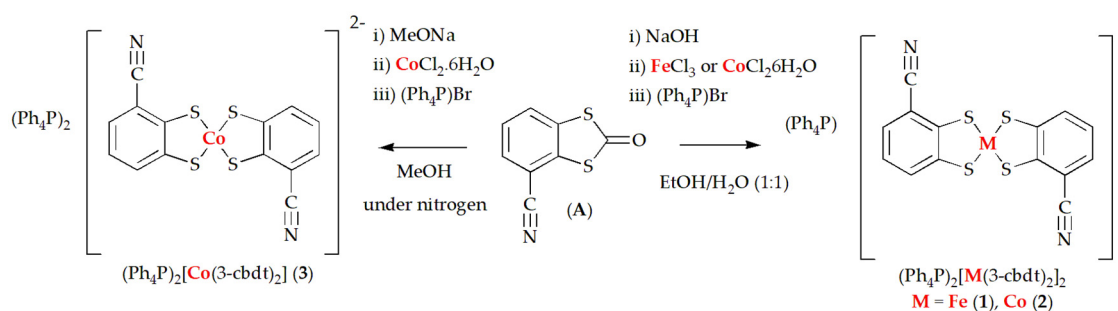


Figure 2. Synthetic route to bis(dithiolene) complexes $[\text{M}(\text{3cbdt})_2]$ $\text{M} = \text{Fe}$ and Co . Reaction conditions: proligand (**A**) cleavage (i); metallic salt for the complexation (ii); cation salt for bis(dithiolate) complex precipitation (iii).

Under anaerobic conditions in methanol solutions, the dianionic Co complex $(\text{Ph}_4\text{P})_2[\text{Co}(\text{3cbdt})_2]$ (**3**) was obtained as needle-shaped orange crystals. Under open atmospheric conditions and in ethanol/water solutions, the monoanionic Fe and Co complexes $(\text{Ph}_4\text{P})_2[\text{M}(\text{3cbdt})_2]$ ($\text{M} = \text{Fe}$ (**1**), Co (**2**)) were obtained. The dianionic Co complex was found to be not stable in solution under open atmospheric conditions and readily oxidizes, with the monoanionic Co complex being obtained upon the recrystallization of the dianionic complex under atmospheric conditions.

3.2. Electrochemical Properties

The redox properties of the Fe and Co complexes were investigated by cyclic voltammetry in acetonitrile and starting from the monoanionic complexes, $(\text{Ph}_4\text{P})_2[\text{M}(\text{3cbdt})_2]$ ($\text{M} = \text{Fe}, \text{Co}$).

A quasi-reversible redox process ascribed to the couple $[\text{M}(\text{3cbdt})_2]^{2-}/[\text{M}(\text{3cbdt})_2]^-$ is observed at -1.08 and -0.826 V (versus Ag/AgNO_3) for $\text{M} = \text{Fe}$ and Co respectively (see Figure S1). These potentials are almost comparable to those observed for the analogs with the ligand 4cbdt and as expected more negative than those observed for the dicyano-substituted ligand dcbdt as shown in Table S1. For the Fe compound, between -0.5 and 0.6 V, we observed an intricate redox process with multiple-step reduction and oxidation

waves that may be due to the redox processes involving dimerized and undimerized species in equilibrium, with the dimer dissociation degree being strongly dependent on the nature of the solvent, as previously described for other Fe bis(dithiolene) complexes [54].

3.3. Crystal and Molecular Structures of the $[M(3cbd\text{t})_2]_2^{2-}$ $M = \text{Fe, Co}$ Complexes

Crystals of **1** and **2** suitable for X-ray diffraction were obtained after recrystallization from CH_2Cl_2 /Hexane. These compounds are isostructural and ORTEP views of the complexes, are depicted in Figure 3a,b. Selected bond lengths and angles for these compounds are presented in Tables S2 and S3.

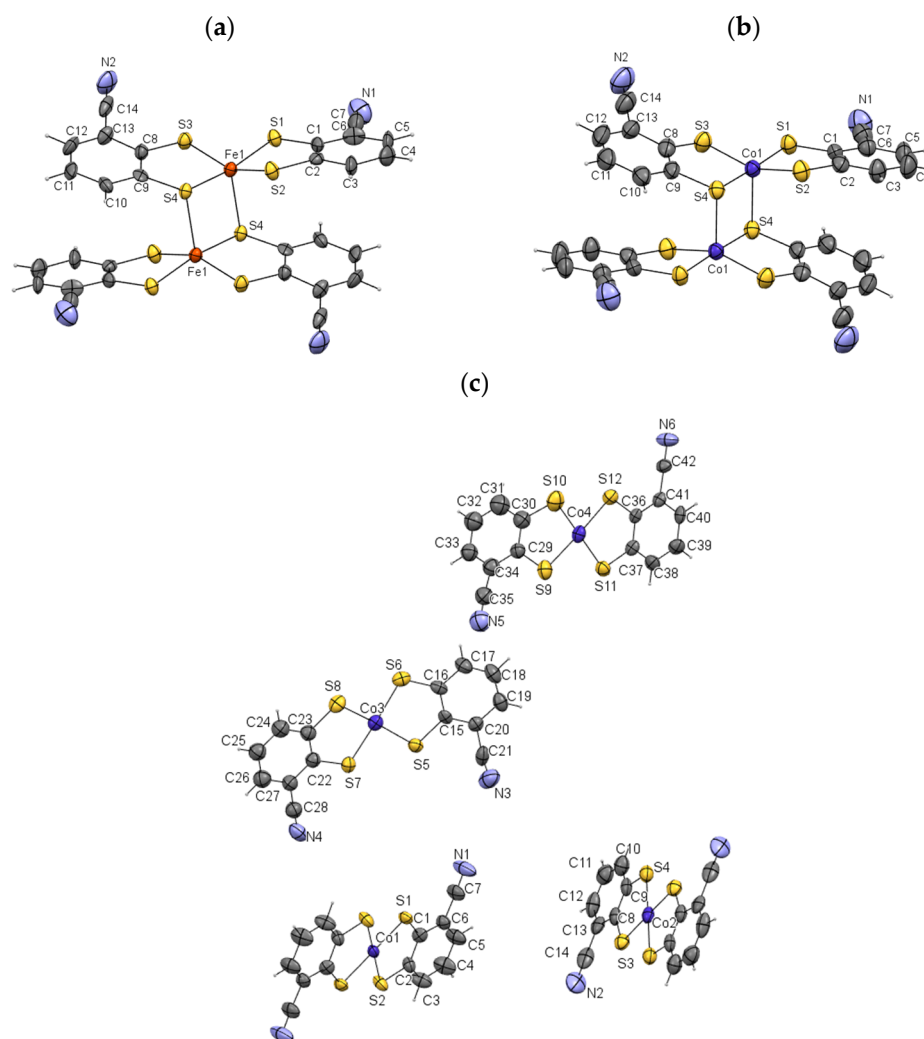


Figure 3. Metal bis(dithiolate) complexes ORTEP diagrams: $(\text{Ph}_4\text{P})_2[\text{Fe}(3\text{cbd}\text{t})_2]_2$ (**1**) (a), $(\text{Ph}_4\text{P})_2\text{Co}(3\text{cbd}\text{t})_2$ (**2**) (b) and $(\text{Ph}_4\text{P})_2[\text{Co}(3\text{cbd}\text{t})_2]$ (**3**) (c). The thermal ellipsoids are drawn at 50% probability and the cations were omitted for clarity.

The asymmetric unit of **1** and **2** contains one Ph_4P^+ cation, one $[M(3\text{cbd}\text{t})_2]^-$ ($M = \text{Fe, Co}$) anion with the CN groups in the cis configuration, and one dichloromethane solvent molecule. The anions present the characteristic dimerization of Fe(III) and Co(III) bis(dithiolenes) forming $[M(3\text{cbd}\text{t})_2]_2^{2-}$ ($M = \text{Fe, Co}$) dimer units with an inversion center between the two metal atoms, which adopt a 4+1 coordination geometry with a metal-over-sulfur overlap mode.

For five-coordinate species, the angular geometric parameter (τ_5) can be defined by the equation $\tau_5 = (\beta - \alpha)/60^\circ$ (where β = the largest angle, α = the second-largest angle around the central atom) [55,56]. In an idealized scenario, this value should be one for trigonal

bipyramidal geometry and zero for square pyramidal geometry. Compound **1** exhibits angles around the Fe central atom, with values of 169.96° for the largest angle (β) and 152.30° for the second-largest angle (α). Compound **2** exhibits angles around the Co central atom, with values of 177.18° for the largest angle (β) and 155.441° for the second-largest angle (α). By applying the above concept, the coordination geometry around the Fe center ($\tau_5 = 0.29$) and around Co center ($\tau_5 = 0.36$) can be more accurately described as distorted square pyramidal rather than trigonal bipyramidal.

The ligands are slightly distorted, repelling each other and making the distance between their mean planes larger than the central M-S distance. The equatorial M-S bond distances (Fe-S1 2.219(2) Å, Fe-S2 2.215(3) Å, Fe-S3 2.217(2) Å, Fe-S4 2.221(2) Å, and Co-S1 2.203(1) Å, Co-S2 2.180(2) Å, Co-S3 2.203(2) Å, Co-S4 2.188(2) Å) and the Fe-S4, Co-S4, apical bonds at 2.461(2) Å, 2.351(1) Å are typical of Fe(III) and Co(III) dimerized complexes, respectively [30,32,33]. The bond lengths of the ligand, namely the S-C and C-C values, are identical to those observed in other similar complexes within the experimental error.

As shown in Figure 4, the crystal structure of these compounds is made up of dimeric anion layers intercalating with cation layers, allowing for anion–anion short $C\equiv N \cdots H-C$ contacts $C(4)-H(4) \cdots N(2)\equiv C(14)$ in both structures—at 2.500 Å and 2.542 Å, for **1** and **2**, respectively—and several other anion–anion interactions slightly longer than the sum of the van der Waals radius (Figure 5).

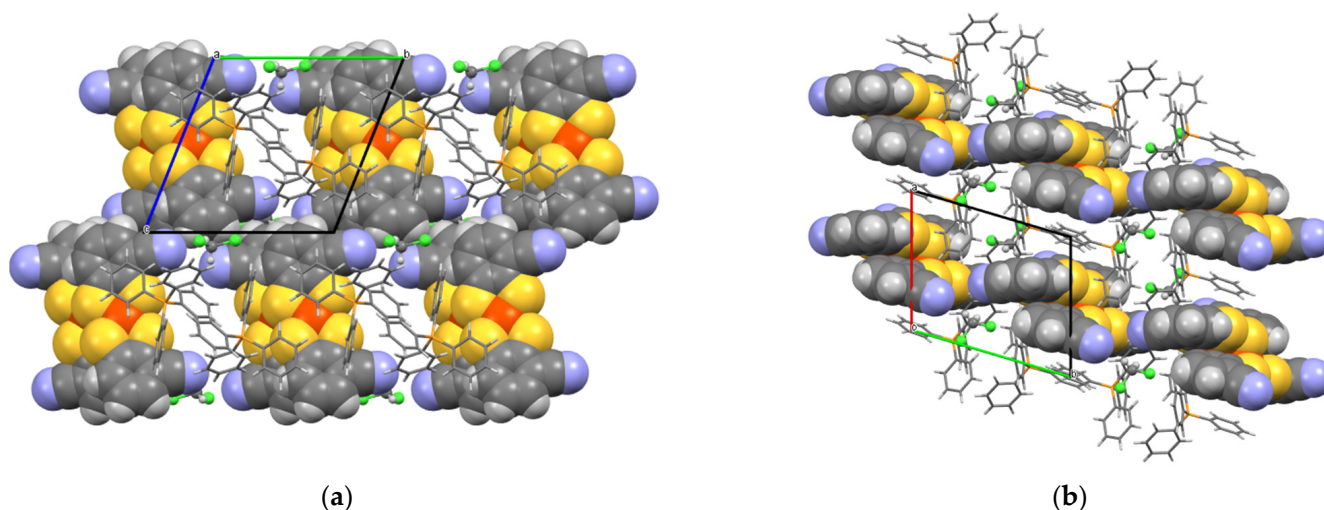


Figure 4. View of a crystal structure of $(Ph_4P)_2[Fe(3cbdt)_2]_2$ (**1**) along the a axis (a) and the c axis (b).

Crystals of **3** suitable for X-ray diffraction were obtained directly from the synthesis and ORTEP view of the complexes, as depicted in Figure 3c. Selected bond lengths and angles for these compounds are presented in Table S4.

The asymmetric unit of **3** contains six Ph_4P^+ cations, one $[Co(3cbdt)_2]^{2-}$ dianion with the CN groups in the cis configuration, another $[Co(3cbdt)_2]^{2-}$ dianion with the CN groups in the trans configuration, and two halves of $[Co(3cbdt)_2]^{2-}$ dianions. In this structure, the dianions present the usual square planar coordination geometry; they are essentially planar with the bond lengths and angles within the expected range for other dianionic bis(dithiolate) Co(II) complexes. The crystal structure is such that the dianions are completely surrounded by cations and there are no short anion–anion contacts. The crystal structure can be described as two mixed anion cation layers (Layer I and Layer II) alternating along the c axis (Figure 6).

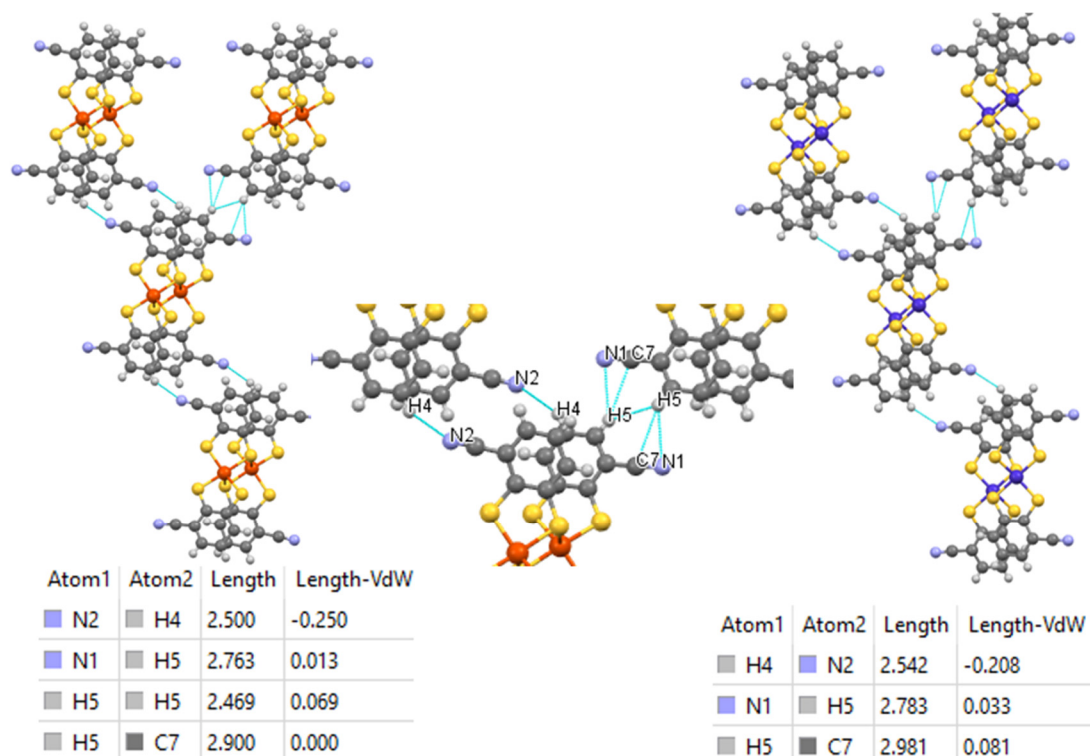


Figure 5. Detail of the anion–anion interactions in compounds $(\text{Ph}_4\text{P})_2[\text{Fe}(\text{3cbdt})_2]_2 \cdot 2\text{CH}_2\text{Cl}_2$ (1) (left) and $(\text{Ph}_4\text{P})_2[\text{Co}(\text{3cbdt})_2]_2 \cdot 2\text{CH}_2\text{Cl}_2$ (2) (right).

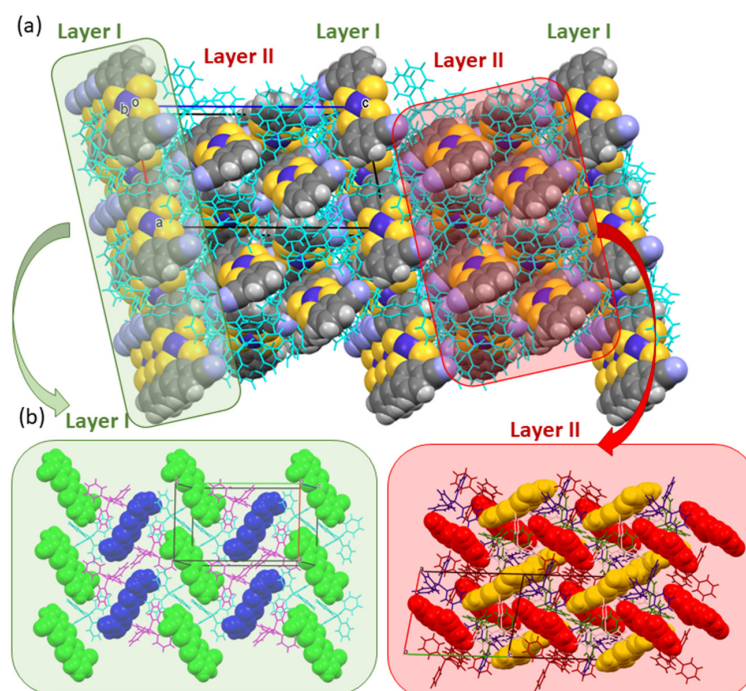


Figure 6. (a) Partial view of the crystal structure of $(\text{Ph}_4\text{P})_2[\text{Co}(\text{3cbdt})_2]_2$ (3), the cations are represented in light wireframe and anions in space fill mode are arranged in two type of layers as shown in (b). The color codes correspond to the symmetrically distinct units.

All the compounds were insulators. The electrical conductivity was measured only at room temperature (see Supplementary Materials).

3.4. Magnetic Properties of the $[M(3cbdt)_2]_2^{2-}$ $M = Fe, Co$ Complexes

The magnetic properties of these compounds were investigated by EPR spectrometry and static magnetic susceptibility measurements in the temperature range 4–300 K.

Concerning monoanionic Co(III) bis(dithiolene) complexes containing a d^6 species, both low-spin $S = 0$ and high-spin $S = 1$ states have been reported depending on the ligand. While most of them are diamagnetic, high-spin states have been described for complexes with some ligands, e.g., substituted benzodithiolates [23,24,57–59].

The Fe(III) complex with a d^5 species is expected to be paramagnetic either in low-spin $S = 1/2$, intermediate-spin $S = 3/2$ or high-spin $S = 5/2$ states. However, upon dimerization, as observed in **1** and **2**, a significant antiferromagnetic interaction between units of the dimer is expected to lead to a diamagnetic ground state, which dominates low-temperature susceptibility, and with excited multiplet states, being thermally accessible can lead to an increasing paramagnetism at higher temperatures.

The iron complex **1** was found to be EPR-silent both at room temperature and 100 K, as was the case with most of the dimerized Fe(III) bis(dithiolene) complexes. However, the magnetic susceptibility measurements show a paramagnetic behavior, with a room temperature susceptibility of 3.8×10^{-3} emu/mol decreasing upon cooling towards a minimum at ~ 28 K $\sim 1.2 \times 10^{-3}$ emu/mol. This was followed by a low temperature increase (Figure 7), which can be ascribed to a Curie tail due to paramagnetic impurities or defects. This behavior is typical of a system of antiferromagnetically coupled dimers with a diamagnetic ground state. The paramagnetic susceptibility data for **1** were fitted considering models of both $S = 1/2$ and $S = 3/2$ dimerized species. The best fit was obtained for $S = 3/2$ using the equation:

$$\chi_P = A + \frac{C}{T} + \frac{2Ng^2\mu_B^2}{kT} \frac{e^{\frac{J}{kT}} + 5e^{\frac{3J}{kT}} + 14e^{\frac{6J}{kT}}}{1 + 3e^{\frac{J}{kT}} + 5e^{\frac{3J}{kT}} + 7e^{\frac{6J}{kT}}} \quad (1)$$

with an antiferromagnetic coupling constant $-J/k_B = 233.6$ K, $g = 1.8$, a temperature independent contribution $A = 9.95 \times 10^{-4}$ emu/mol, and $C = 0.013$ emu K/mol, which corresponds to approximately 0.7% of $S = 3/2$ impurities. These parameters are identical to those reported for other dimerized Fe(III) bis(dithiolene) complexes where the $S = 3/2$ model has been found in most cases as the most appropriated [33,60,61].

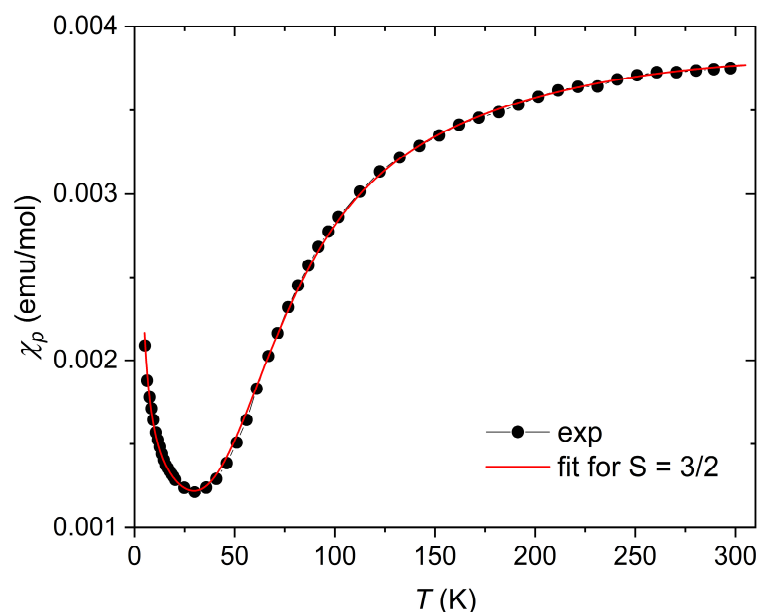


Figure 7. Paramagnetic susceptibility χ of $(\text{Ph}_4\text{P})_2[\text{Fe}(3\text{cbdt})_2]_2$ (**1**) as a function of the temperature T . The dashed line is a fit by Equation (1), considering dimers of $S = 3/2$ spins (see text).

The dianionic Co(II) complex, $(\text{Ph}_4\text{P})_2[\text{Co}(\text{3cbdt})_2]$ (**3**), as expected for a d^7 species, was found to be paramagnetic with an almost temperature-independent effective magnetic moment of $\mu_{\text{eff}} \sim 2 \mu_{\text{B}}$ above 25 K (Figure 8). This value is close to the one expected for a spin-only value $S = 1/2$ system, with $g = 2.0$ ($\mu_{\text{S}} = 1.73 \mu_{\text{B}}$ and $\mu_{\text{eff}} = 1.8 \mu_{\text{B}}$ considering spin-orbit coupling usually found in Co complexes), which is identical to those reported for other Co(II) bis(dithiolene) complexes such as $[\text{Co}(\text{dcbdt})_2]^{2-}$ [24].

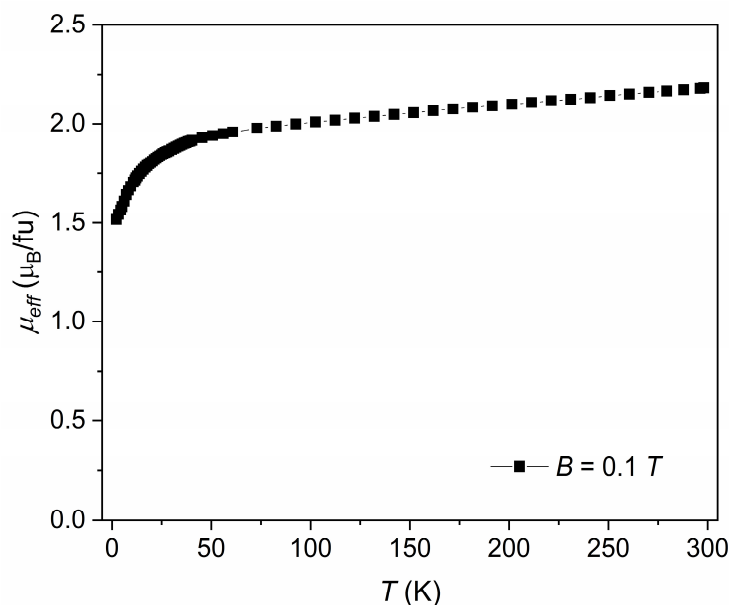


Figure 8. Effective magnetic moment μ_{eff} of $(\text{Ph}_4\text{P})_2[\text{Co}(\text{3cbdt})_2]$ (**3**), as a function of the temperature T .

The paramagnetic nature of **3** was confirmed by EPR spectrometry, showing (Figure 9) a rhombic system with eight lines partially resolved in the g_z region due to the interaction with the ^{59}Co nuclear spin $I = 7/2$ [62–64]. This hyperfine structure is usually observed only in diluted systems when there is a large separation between the complexes reducing the effects of dipolar interactions, and this is a rare example of such a situation for a pure compound in the solid state due to the large separation between the Co complexes by the cations, with the smallest Co-Co distance being 10.794 Å. The simulation of the spectra was conducted with the following parameters: $g_{xx} = 1.938$, $g_{yy} = 2.098$, $g_{zz} = 3.036$, $A_{xx}(^{59}\text{Co}) = 10$ MHz, $A_{yy}(^{59}\text{Co}) = 190$ MHz, $A_{zz}(^{59}\text{Co}) = 356$ MHz, (linewidth using $g\text{strain}_{xx} = 0.12$, $g\text{strain}_{yy} = 0.10$ and $g\text{strain}_{zz} = 0.14$). The observed spectrum is quite similar to those observed in the salts of $[\text{Co}(\text{cbdt})_2]^{2-}$ and $[\text{Co}(\text{dcbdt})_2]^{2-}$, where the hyperfine interaction was found to be around 300 MHz [24,34,65].

The Co(III) dimerized compound $(\text{Ph}_4\text{P})_2[\text{Co}(\text{3cbdt})_2]_2$ (**2**) was found to be EPR-silent at room temperature and at 100 K. A possible high-spin state for the Co(III) is denoted by the static magnetic susceptibility measurements (Figure 10), which in addition to a low-temperature Curie tail, show a modest but significant increase in paramagnetic susceptibility above 100 K, which can be ascribed to the multiplet states becoming increasingly thermally accessible from the singlet ground state. However, this modest increase in susceptibility is indicative of dimer antiferromagnetic coupling J significantly larger than room temperature. A good fit of the dimer equation below, which describes the susceptibility for dinuclear homospin system with $S = 1$ (singlet-quintet model), was obtained with $J/k_B \approx -1286$ K.

$$\chi_p = A + \frac{C}{T} + \frac{2Ng^2\mu_B^2}{kT} \frac{\exp\left(\frac{J}{kT}\right) + 5\left(\exp\frac{3J}{kT}\right)}{1 + 3\exp\left(\frac{J}{kT}\right) + 5\exp\left(\frac{3J}{kT}\right)} \quad (2)$$

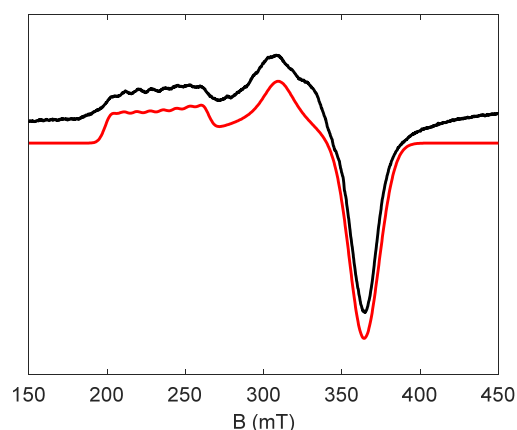


Figure 9. Experimental (black) and simulated (red) EPR spectra of $(\text{Ph}_4\text{P})_2[\text{Co}(\text{3cbdt})_2]$ (3) as a polycrystalline sample at room temperature. Experimental conditions: 9.3155 GHz, power of 4.9 mW and a modulation of 0.4 mT. Simulation parameters are given in the text.

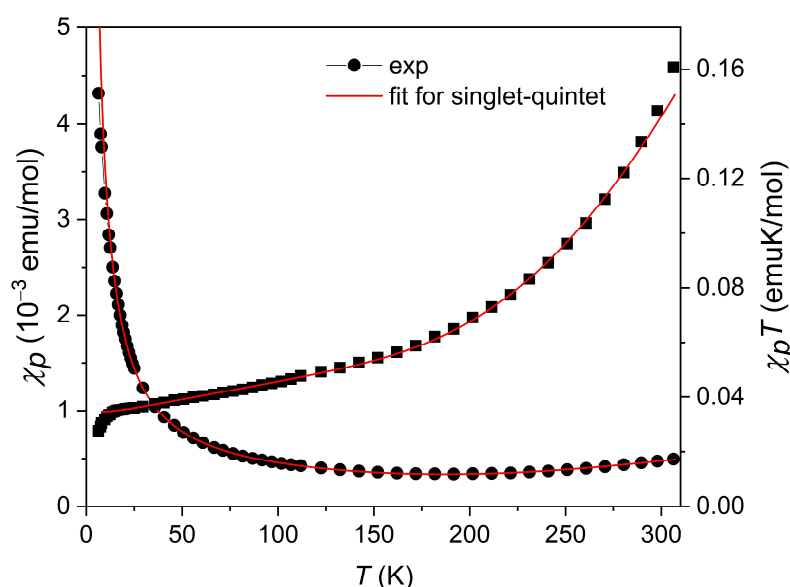


Figure 10. Temperature dependence of the paramagnetic susceptibility of $(\text{Ph}_4\text{P})_2[\text{Co}(\text{3cbdt})_2]_2$ (2).

4. Conclusions

In this work, we reported three new compounds: two bis(dithiolene) complexes obtained in the monoanionic state— $[\text{M}(\text{3cbdt})_2]^-$ with $\text{M} = \text{Fe}$ and Co —and one bis(dithiolene) complex obtained in the dianionic state: $[\text{M}(\text{3cbdt})_2]^{2-}$ with $\text{M} = \text{Co}$. The monoanionic complexes of Co and Fe both exhibit typical dimerization, featuring a 4 + 1 metal coordination geometry ($[\text{M}(\text{3cbdt})_2]_2^{2-}$ ($\text{M} = \text{Fe}$ and Co)). The coordination geometry around the Fe center ($\tau_5 = 0.29$) and the Co center ($\tau_5 = 0.36$) is distorted and square pyramidal. The dimerized monoanionic $\text{Co}(\text{III})$ complex ($[\text{Co}(\text{3cbdt})_2]_2^{2-}$) is EPR-silent and is an example of a cobalt complex with a high-spin $S = 1$ ground state. The $\text{Co}(\text{II})$ dianionic complex ($[\text{Co}(\text{3cbdt})_2]^{2-}$) is a paramagnetic $S = 1/2$ system and a rare example showing, in the solid-state EPR, the hyperfine structure of the $I(^{59}\text{Co}) = 7/2$. The dimerized monoanionic $\text{Fe}(\text{III})$ complex ($[\text{Fe}(\text{3cbdt})_2]_2^{2-}$) was found to be EPR-silent, as was the case with most of the dimerized $\text{Fe}(\text{III})$ bis(dithiolene) complexes. The magnetic susceptibility measurements show a paramagnetic behavior typical of antiferromagnetically coupled $S = 3/2$ species with a coupling constant of $-J/k_B = 233.6$ K.

Supplementary Materials: The following supporting information can be downloaded at: <https://www.mdpi.com/article/10.3390/cryst14050469/s1>, Figure S1: Cyclic voltammograms of

[Ph₄P][Fe(3cbdt)₂] (top) and [Ph₄P][Co(3cbdt)₂] (bottom) in CH₃CN with [n-Bu₄N][PF₆] 0.1 M as electrolyte, V vs. Ag/Ag⁺, scan rate 100 mV s⁻¹.; Table S1: Redox potentials of [M(L)₂]²⁻/[M(L)₂]⁻, M=Co, Fe; L=3-cbdt and 4-cbdt in acetonitrile (ref. Ag/AgNO₃); Table S2: Bond lengths [Å] and angles [deg] for compound 1; Table S3: Bond lengths [Å] and angles [deg] for compound 2; Table S4: Bond lengths [Å] and angles [deg] for compound 3; electrical transport measurements.

Author Contributions: S.R. was responsible for the original conceptualization of this work. The manuscript was prepared based on research contributions from all the authors in different topics, namely A.G.C., G.L., J.F.G.R. and D.S. concerning sample preparation, I.C.S. and A.G.C. the structural analysis, E.B.L. the electrical transport measurements, L.C.J.P. and A.G.C. the magnetic characterization discussion and final review, N.L.B. and S.C. the EPR measurements and discussion. S.R., S.A.B. and M.A. ensured funding acquisition and the final review and editing of the manuscript. All authors have read and agreed to the published version of the manuscript.

Funding: This work was supported by Fundação para a Ciência e a Tecnologia (FCT) through UID/Multi/04349/2019, the National Infrastructure Roadmap, LTHMFL-NECL LISBOA-01-0145-FEDER-022096, RNEM—Portuguese Mass Spectrometry Network, LISBOA-01-0145-FEDER-022125, also funded by the Lisboa Regional Operational Program (Lisboa2020) under the PT2020 Partnership Agreement, via the European Regional Development Fund (ERDF). The collaboration between the Portuguese and French team members was supported by the “PHC PESSOA” programme (project number: 47836RH), funded by the French Ministry for Europe and Foreign Affairs, the French Ministry for Higher Education and Research and the Portuguese FCT.

Data Availability Statement: The data supporting the conclusions of this article will be made available by the authors on request.

Acknowledgments: Financial support from the CNRS and the University of Strasbourg is gratefully acknowledged.

Conflicts of Interest: The authors declare no conflict of interest.

References

1. Gray, H.B.; Billig, E.; Williams, R.; Bernal, I. A Spin-Free Square Planar Cobaltous Complex. *J. Am. Chem. Soc.* **1962**, *84*, 3596–3597. [[CrossRef](#)]
2. Robertson, N.; Cronin, L. Metal bis-1,2-dithiolene complexes in conducting or magnetic crystalline assemblies. *Coord. Chem. Rev.* **2002**, *227*, 93–127. [[CrossRef](#)]
3. Kato, R. Conducting metal dithiolene complexes: Structural and electronic properties. *Chem. Rev.* **2004**, *104*, 5319–5346. [[CrossRef](#)] [[PubMed](#)]
4. Eisenberg, R.; Gray, H.B. Noninnocence in Metal Complexes: A Dithiolene Dawn. *Inorg. Chem.* **2011**, *50*, 9741–9751. [[CrossRef](#)] [[PubMed](#)]
5. Coucouvanis, D. The Chemistry of the Dithioacid and 1,1-Dithiolate Complexes. In *Progress in Inorganic Chemistry*; Wiley Online Library: Hoboken, NJ, USA, 1970; pp. 233–371. [[CrossRef](#)]
6. Ke, S.W.; Wang, Y.D.; Su, J.; Liao, K.; Lv, S.; Song, X.M.; Ma, T.R.; Yuan, S.; Jin, Z.; Zuo, J.L. Redox-Active Covalent Organic Frameworks with Nickel-Bis(dithiolene) Units as Guiding Layers for High-Performance Lithium Metal Batteries. *J. Am. Chem. Soc.* **2022**, *144*, 8267–8277. [[CrossRef](#)] [[PubMed](#)]
7. Olubummo, A.; Zhao, L.H.; Hartman, A.; Tom, H.; Zhao, Y.; Wycoff, K. Photothermal bleaching of nickel dithiolene for bright multi-colored 3D printed parts. *Nat. Commun.* **2023**, *14*, 586. [[CrossRef](#)] [[PubMed](#)]
8. Zhang, P.; Hou, X.L.; Liu, L.; Mi, J.L.; Dong, M.D. Two-Dimensional pi-Conjugated Metal Bis(dithiolene) Complex Nanosheets as Selective Catalysts for Oxygen Reduction Reaction. *J. Phys. Chem. C* **2015**, *119*, 28028–28037. [[CrossRef](#)]
9. Fontinha, D.; Sousa, S.A.; Morais, T.S.; Prudencio, M.; Leitao, J.H.; Le Gal, Y.; Lorcy, D.; Silva, R.A.L.; Velho, M.F.G.; Belo, D.; et al. Gold(III) bis(dithiolene) complexes: From molecular conductors to prospective anticancer, antimicrobial and antiplasmodial agents. *Metallomics* **2020**, *12*, 974–987. [[CrossRef](#)] [[PubMed](#)]
10. Chen, K.; Fang, W.J.; Zhang, Q.Y.; Jiang, X.Y.; Chen, Y.; Xu, W.J.; Shen, Q.M.; Sun, P.F.; Huang, W. Tunable NIR Absorption Property of a Dithiolene Nickel Complex: A Promising NIR-II Absorption Material for Photothermal Therapy. *ACS Appl. Bio Mater.* **2021**, *4*, 4406–4412. [[CrossRef](#)]
11. Camerel, F.; Fourmigue, M. (Photo)Thermal Stimulation of Functional Dithiolene Complexes in Soft Matter. *Eur. J. Inorg. Chem.* **2020**, *2020*, 508–522. [[CrossRef](#)]
12. Wu, Z.Z.; Adekoya, D.; Huang, X.; Kiefel, M.J.; Xie, J.; Xu, W.; Zhang, Q.C.; Zhu, D.B.; Zhang, S.Q. Highly Conductive Two-Dimensional Metal-Organic Frameworks for Resilient Lithium Storage with Superb Rate Capability. *ACS Nano* **2020**, *14*, 12016–12026. [[CrossRef](#)] [[PubMed](#)]

13. Xie, L.S.; Skorupskii, G.; Dinca, M. Electrically Conductive Metal-Organic Frameworks. *Chem. Rev.* **2020**, *120*, 8536–8580. [[CrossRef](#)] [[PubMed](#)]
14. Kobayashi, Y.; Jacobs, B.; Allendorf, M.D.; Long, J.R. Conductivity, Doping, and Redox Chemistry of a Microporous Dithiolene-Based Metal-Organic Framework. *Chem. Mater.* **2010**, *22*, 4120–4122. [[CrossRef](#)]
15. Sousa, A.; Santos, J.F.; Silva, F.; Sousa, S.A.; Leitão, J.H.; Matos, A.P.; Pinheiro, T.; Silva, R.A.L.; Belo, D.; Almeida, M.; et al. Antitumoral and Antimicrobial Activities of Block Copolymer Micelles Containing Gold Bisdithiolate Complexes. *Pharmaceutics* **2023**, *15*, 564. [[CrossRef](#)] [[PubMed](#)]
16. Vlcek, A. Dithiolenes and non-innocent redox-active ligands. *Coord. Chem. Rev.* **2010**, *254*, 1357–1588. [[CrossRef](#)]
17. McCleverty, J.A. Metal 1,2-Dithiolene and Related Complexes. *Prog. Inorg. Chem.* **1968**, *10*, 49–221. [[CrossRef](#)]
18. Belo, D.; Alves, H.; Lopes, E.B.; Duarte, M.T.; Gama, V.; Henriques, R.T.; Almeida, M.; Perez-Benitez, A.; Rovira, C.; Veciana, J. Gold complexes with dithiothiophene ligands: A metal based on a neutral molecule. *Chem. Eur. J.* **2001**, *7*, 511–519. [[CrossRef](#)] [[PubMed](#)]
19. Tanaka, H.; Okano, Y.; Kobayashi, H.; Suzuki, W.; Kobayashi, A. A three-dimensional synthetic metallic crystal composed of single-component molecules. *Science* **2001**, *291*, 285–287. [[CrossRef](#)] [[PubMed](#)]
20. Velho, M.F.G.; Silva, R.A.L.; Belo, D. The quest for single component molecular metals within neutral transition metal complexes. *J. Mater. Chem. C* **2021**, *9*, 10591–10609. [[CrossRef](#)]
21. Simao, D.; Ayllon, J.A.; Rabaca, S.; Figueira, M.J.; Santos, I.C.; Henriques, R.T.; Almeida, M. Fe(qdt)₂(-)- salts; an undimerised Fe-III bis(dithiolene) complex stabilised by cation interactions. *Crystengcomm* **2006**, *8*, 658–661. [[CrossRef](#)]
22. Yu, R.; Arumugam, K.; Manepalli, A.; Tran, Y.; Schmehl, R.; Jacobsen, H.; Donahue, J.P. Reversible, electrochemically controlled binding of phosphine to iron and cobalt bis(dithiolene) complexes. *Inorg. Chem.* **2007**, *46*, 5131–5133. [[CrossRef](#)] [[PubMed](#)]
23. Eisenberg, R. *Structural Systematics of 1,1- and 1,2-Dithiolato Chelates*; John Wiley & Sons Ltd.: Hoboken, NJ, USA, 1970. [[CrossRef](#)]
24. Alves, H.; Simao, D.; Santos, I.C.; Gama, V.; Henriques, R.T.; Novais, H.; Almeida, M. A series of transition metal bis(dicyanobenzenedithiolate) complexes [M(dcbdt)₂] (M = Fe, Co, Ni, Pd, Pt, Cu, Au and Zn). *Eur. J. Inorg. Chem.* **2004**, *2004*, 1318–1329. [[CrossRef](#)]
25. Gama, V.; Henriques, R.T.; Almeida, M.; Veiros, L.; Calhorda, M.J.; Meetsma, A.; Deboer, J.L. A novel trinuclear cobalt complex crystal and electronic structure of (Per)₄[Co(mnt)₂]₃. *Inorg. Chem.* **1993**, *32*, 3705–3711. [[CrossRef](#)]
26. Gama, V.; Henriques, R.T.; Bonfait, G.; Almeida, M.; Meetsma, A.; Vansmaalen, S.; Deboer, J.L. (Perylene)Co(mnt)₂(CH₂Cl₂)_{0.5}: A mixed perylenecobalt complex as molecular and polymeric conductor. *J. Am. Chem. Soc.* **1992**, *114*, 1986–1989. [[CrossRef](#)]
27. Simao, D.; Alves, H.; Belo, D.; Rabaca, S.; Lopes, E.B.; Santos, I.C.; Gama, V.; Duarte, M.T.; Henriques, R.T.; Novais, H.; et al. Synthesis, structure and physical properties of tetrabutylammonium salts of nickel complexes with the new ligand dcbdt = 4,5-dicyanobenzene-1,2-dithiolate, [Ni(dcbdt)₂](z-) (z = 0.4, 1, 2). *Eur. J. Inorg. Chem.* **2001**, *2001*, 3119–3126. [[CrossRef](#)]
28. Alves, H.; Simao, D.; Lopes, E.B.; Belo, D.; Gama, V.; Duarte, M.T.; Novais, H.; Henriques, R.T.; Almeida, M. Structure and physical properties of (n-Bu₄N)₂[Au(dcbdt)₂]₅. *Synth. Met.* **2001**, *120*, 1011–1012. [[CrossRef](#)]
29. Alves, H.; Simao, D.; Santos, I.C.; Lopes, E.B.; Novais, H.; Henriques, R.T.; Almeida, M. Charge transfer salts based on M(dcbdt)₂ complexes (M = Au and Ni). *Synth. Met.* **2003**, *135–136*, 543–544. [[CrossRef](#)]
30. Alves, H.; Simao, D.; Novais, H.; Santos, I.C.; Gimenez-Saiz, C.; Gama, V.; Waerenborgh, J.C.; Henriques, R.T.; Almeida, M. (n-Bu₄N)₂[Fe(dcbdt)₂]₂. Synthesis, crystal structure and magnetic characterisation. *Polyhedron* **2003**, *22*, 2481–2486. [[CrossRef](#)]
31. Alves, H.; Santos, I.C.; Lopes, E.B.; Belo, D.; Gama, V.; Simao, D.; Novais, H.; Duarte, M.T.; Henriques, R.T.; Almeida, M. Conductors based on metal-bisdicyanobenzodithiolate complexes. *Synth. Met.* **2003**, *133–134*, 397–399. [[CrossRef](#)]
32. Lopes, E.B.; Alves, H.; Santos, I.C.; Graf, D.; Brooks, J.S.; Canadell, E.; Almeida, M. The family of molecular conductors [(n-Bu)₄N]₂[M(dcbdt)₂]₅, M = Cu, Ni, Au; band filling and stacking modulation effects. *J. Mater. Chem.* **2008**, *18*, 2825–2832. [[CrossRef](#)]
33. Cerdeira, A.C.; Simao, D.; Santos, I.C.; Machado, A.; Pereira, L.C.J.; Waerenborgh, J.C.; Henriques, R.T.; Almeida, M. (n-Bu₄N)[Fe(cbdt)₂]: Synthesis, crystal structure and magnetic characterisation of a new Fe-III bis(dithiolene) complex. *Inorganica Chim. Acta* **2008**, *361*, 3836–3841. [[CrossRef](#)]
34. Cerdeira, A.C.; Afonso, M.L.; Santos, I.C.; Pereira, L.C.J.; Coutinho, J.T.; Rabaca, S.; Simao, D.; Henriques, R.T.; Almeida, M. Synthesis, structure and physical properties of transition metal bis 4-cyanobenzene-1,2-dithiolate complexes [M(cbdt)₂]^{z-} (M = Zn, Co, Cu, Au, Ni, Pd, z = 0, 1, 2). *Polyhedron* **2012**, *44*, 228–237. [[CrossRef](#)]
35. Oliveira, S.; Belo, D.; Santos, I.C.; Rabaca, S.; Almeida, M. Synthesis and characterization of the cyanobenzene-ethylenedithio-TTF donor. *Beilstein J. Org. Chem.* **2015**, *11*, 951–956. [[CrossRef](#)]
36. Oliveira, S.; Ministro, J.; Santos, I.C.; Belo, D.; Lopes, E.B.; Rabaça, S.; Canadell, E.; Almeida, M. Bilayer molecular metals based on dissymmetrical electron donors. *Inorg. Chem.* **2015**, *54*, 6677–6679. [[CrossRef](#)]
37. Lopes, G.; da Gama, V.; Belo, D.; Simao, D.; Santos, I.C.; Almeida, M.; Rabaca, S. A 4-cyanobenzene-ethylenedithio-TTF electron donor and its (1:1) triiodide radical cation salt; isomer effects in C-N center dot center dot center dot H-C interactions. *Crystengcomm* **2019**, *21*, 637–647. [[CrossRef](#)]
38. Rabaca, S.; Almeida, M. Dithiolene complexes containing N coordinating groups and corresponding tetrathiafulvalene donors. *Coord. Chem. Rev.* **2010**, *254*, 1493–1508. [[CrossRef](#)]
39. Jeannin, O.; Delaunay, J.; Barriere, F.; Fourmigue, M. Between Ni(mnt)₂ and Ni(tfd)₂ dithiolene complexes: The unsymmetrical 2-(trifluoromethyl)acrylonitrile-1,2-dithiolate and its nickel complexes. *Inorg. Chem.* **2005**, *44*, 9763–9770. [[CrossRef](#)]

40. Ruffin, H.; Baudron, S.A.; Salazar-Mendoza, D.; Hosseini, M.W. A Silver Bite: Crystalline Heterometallic Architectures Based on Ag- p Interactions with a Bis- Dipyrin Zinc Helicate. *Chem. Eur. J.* **2014**, *20*, 2449–2453. [[CrossRef](#)]
41. Baudron, S.A. Dipyrin based homo- and hetero-metallic infinite architectures. *Crystengcomm* **2010**, *12*, 2288–2295. [[CrossRef](#)]
42. Fenton, H.; Tidmarsh, I.S.; Ward, M.D. Hierarchical self-assembly of heteronuclear co-ordination networks. *Dalton Trans.* **2010**, *39*, 3805–3815. [[CrossRef](#)]
43. Kremer, M.; Englert, U. N Donor substituted acetylacetonones ditopic ligands versatile. *Z. Fur Krist.-Cryst. Mater.* **2018**, *233*, 437–452. [[CrossRef](#)]
44. Kumar, G.; Gupta, R. Molecularly designed architectures—The metalloligand way. *Chem. Soc. Rev.* **2013**, *42*, 9403–9453. [[CrossRef](#)] [[PubMed](#)]
45. Santos, I.C.; Gama, V.; Rabaca, S.; Veiros, L.F.; Nogueira, F.; Paixao, J.A.; Almeida, M. Structural diversity in conducting bilayer salts (CNB-EDT-TTF)₄A. *Crystengcomm* **2020**, *22*, 8313–8321. [[CrossRef](#)]
46. Costa, A.G.; Lopes, G.; Ribeiro, S.; Santos, I.C.; Simao, D.; Pereira, L.C.J.; Le Breton, N.; Choua, S.; Baudron, S.A.; Almeida, M.; et al. Cyano benzene functionalised Ni and Cu bis(dithiolene) complexes. *Crystengcomm* **2023**, *25*, 5362–5371. [[CrossRef](#)]
47. *Bruker Apex3, Crystallography Software Suite*; Bruker Axs Inc.: Madison, WI, USA, 2016.
48. *Bruker Axs: Saint+, Release 6.22. Bruker AXS:SAINT+, Release 622*; Bruker Analytical Systems: Madison, WI, USA, 2005.
49. *Bruker Axs: Sadabs. Bruker AXS:SADABS*; Bruker Analytical Systems: Madison, WI, USA, 2005.
50. Sheldrick, G.M. A short history of SHELX. *Acta Crystallogr. A-Found. Adv.* **2008**, *64*, 112–122. [[CrossRef](#)] [[PubMed](#)]
51. Sheldrick, G.M. Crystal structure refinement with SHELXL. *Acta Crystallogr. Sect. C-Struct. Chem.* **2015**, *71*, 3–8. [[CrossRef](#)] [[PubMed](#)]
52. Farrugia, L.J. WinGX and ORTEP for Windows: An update. *J. Appl. Crystallogr.* **2012**, *45*, 849–854. [[CrossRef](#)]
53. Macrae, C.F.; Sovago, I.; Cottrell, S.J.; Galek, P.T.A.; McCabe, P.; Pidcock, E.; Platings, M.; Shields, G.P.; Stevens, J.S.; Towler, M.; et al. Mercury 4.0: From visualization to analysis, design and prediction. *J. Appl. Crystallogr.* **2020**, *53*, 226–235. [[CrossRef](#)] [[PubMed](#)]
54. Afonso, M.L.; Neves, A.I.S.; Almeida, M. Dimerisation of Fe bis(dithiolene) complexes: An electrochemical study. *Inorganica Chim. Acta* **2015**, *426*, 160–164. [[CrossRef](#)]
55. Baker-Hawker, M.J.; Billig, E.; Gray, H.B. Characterization and Electronic Structures of Metal Complexes Containing Benzene-1,2-dithiolate and Related Ligands. *J. Am. Chem. Soc.* **1966**, *88*, 4870–4875. [[CrossRef](#)]
56. Addison, A.W.; Rao, T.N.; Reedijk, J.; Van Rijn, J.; Verschoor, G.C. Synthesis, structure, and spectroscopic properties of copper(II) compounds containing nitrogen-sulfur donor ligands: The crystal and molecular structure of aqua[1,7-bis(N-methylbenzimidazol-2'-yl)-2,6-dithiaheptane]copper(II) perchlorate. *J. Chem. Soc. Dalton Trans. Inorg. Chem.* **1984**, *7*, 1972–1999. [[CrossRef](#)]
57. Blackman, A.G.; Schenk, E.B.; Jelley, R.E.; Krensked, E.H.; Gahan, L.R. Five-coordinate transition metal complexes and the value of τ_5 : Observations and caveats. *Dalton Trans.* **2020**, *49*, 14798–14806. [[CrossRef](#)] [[PubMed](#)]
58. Van der Put, P.J.; Schilperoord, A.A. Spin delocalization in square-planar spin-triplet benzene- and toluenedithiolatecobaltate(III). *Inorg. Chem.* **1974**, *13*, 2476–2481. [[CrossRef](#)]
59. Silva, R.A.L.; Santos, R.; Andrade, M.M.; Santos, I.C.; Coutinho, J.T.; Pereira, L.C.J.; Waerenborgh, J.C.; Vieira, B.J.C.; Cirera, J.; Ruiz, E.; et al. Co/Fe(α -Alkyl-tpdt)₂^{X-}: Alkyl-Substituted Cobalt and Iron Bis-dithiolenethiophenic Complexes. *Inorg. Chem.* **2020**, *59*, 9261–9269. [[CrossRef](#)] [[PubMed](#)]
60. Gama, V.; Henriques, R.T.; Bonfait, G.; Pereira, L.C.; Waerenborgh, J.C.; Santos, I.C.; Duarte, M.T.; Cabral, J.M.P.; Almeida, M. Low-dimensional molecular metals bis(maleonitriledithiolato)bis(perylene)metal, metal = iron and cobalt. *Inorg. Chem.* **1992**, *31*, 2598–2604. [[CrossRef](#)]
61. Rodrigues, J.V.; Santos, I.C.; Gama, V.; Henriques, R.T.; Waerenborgh, J.C.; Duarte, M.T.; Almeida, M. Synthesis, structure and properties of [Hpy]₂[M(mnt)₂]₂ (M = Co or Fe, Hpy = pyridinium, mnt = maleonitriledithiolate). *J. Chem. Soc. Dalton Trans.* **1994**, 2655–2660. [[CrossRef](#)]
62. Weil, J.A.; Bolton, J.R.; Wertz, J.E. *Electron Spin Resonance: Elementary Theory and Practical Applications*; Springer Science & Business Media: New York, NY, USA, 1994.
63. Walker, F.A.; Bowen, J. EPR evidence for hydrogen bond donation to the terminal oxygen of cobalt-oxygen model compounds and cobalt oxymyoglobin. *J. Am. Chem. Soc.* **1985**, *107*, 7632–7635. [[CrossRef](#)]
64. Hoffman, B.M.; Diemente, D.L.; Basolo, F. Electron paramagnetic resonance studies of some cobalt(II) Schiff base compounds and their monomeric oxygen adducts. *J. Am. Chem. Soc.* **1970**, *92*, 61–65. [[CrossRef](#)]
65. Bill, E.; Bothe, E.; Chaudhuri, P.; Chlopek, K.; Herebian, D.; Kokatam, S.; Ray, K.; Weyhermüller, T.; Neese, F.; Wiegardt, K. Molecular and Electronic Structure of Four- and Five-Coordinate Cobalt Complexes Containing Two *o*-Phenylenediamine- or Two *o*-Aminophenol-Type Ligands at Various Oxidation Levels: An Experimental, Density Functional, and Correlated ab initio Study. *Chem. Eur. J.* **2005**, *11*, 204–224. [[CrossRef](#)] [[PubMed](#)]

Disclaimer/Publisher's Note: The statements, opinions and data contained in all publications are solely those of the individual author(s) and contributor(s) and not of MDPI and/or the editor(s). MDPI and/or the editor(s) disclaim responsibility for any injury to people or property resulting from any ideas, methods, instructions or products referred to in the content.